NUMERICAL MODELING AND EXPERIMENTAL INVESTIGATION OF THE SUPERFICIAL LAYER OF SKD61 STEEL DURING LASER SURFACE HARDENING

Kwo-An Chiang* and Yong-Chwang Chen

ABSTRACT

Laser heating of SKD61 steel usually causes the formation of a melting layer on the steel surface, which is of poor thermal conductivity and diffusivity. The modified Ashby-Easterling heat-transfer equation was used to simulate the temperature distribution for laser surface hardening of SKD61 steel. The phase transformation temperatures of SKD61 in the quenched and as-received conditions were compared with each other for different laser energy densities. When the laser was focused on the steel, the temperature of the SKD61 was raised. Due to the effect of superheating, the critical phase transformation temperature in laser hardening became higher than the austenized temperature (1010°C) in traditional quenching. However, the critical phase transformation temperature of SKD61 decreased with increasing laser energy density.

Key Words: laser transformation hardening, dendrites, temperature distribution field, austenite.

I.INTRODUCTION

High-energy density beam processing is a special technology that utilizes a high-energy density beam (e.g., a laser beam, electronic beam, or plasma) as a heat source for such applications as welding, incision, punching, spray painting, surface treatment, etching, and fine machining (Yang *et al*., 2001). All of these processes have been studied both theoretically and experimentally (Mazumder and Steen,1980; Steen, 2003; Bokota and Iskierka, 1996). Surface treatments effected by laser beam irradiation include laser hardening, laser alloying, and laser cladding. The common feature of all of these processes is the production of certain thermal cycles in small, highly localized regions on the surface of the work-piece, which take on new properties that allow them to cope better with wear, fatigue, and corrosion while maintaining most of their original properties.

Industrial applications of laser surface treatment have become popular because it has the advantages of using high power density, but, low heat input; and it provides a thin hardening layer as well as a small heat-affected zone (Ganeev, 2002; Olaineck, 1996). The popularity is especially prevalent for laser surface hardening of high-end technological products. Recent reviews of the principles and applications of laser treatments describe the use of lasers as a controlled heat source for transformation hardening. The classical approach to modeling the heat flow induced by a distributed heat source moving over the surface of a semi-infinite solid starts with the solution for a point source and then integrates it over the area of the beam. This widely used method requires numerical procedures for its evaluation, as do the finite difference solutions of Kou and co-workers (Kou *et al*., 1983). They developed a 3-D heat model and varied the beam power and traverse speed. Then, they performed dimensional analysis of heat flow during heat treating and melting. However, the results were not easy to determine for complex shapes and needed complicated calculation. Another approach to heat flow modeling applied to a moving heat source by Rosenthal and several other authors has used the finite-element method for numerical evaluation, as do the FEM analyses of Pavelic and co-workers (Goldak *et al*., 1984). The FEM analysis allows variation of

*Corresponding author. (Tel: 886-2-23684463; Fax: 886-2-23625489; Email: d89522007@ntu.edu.tw)

The authors are with the Department of Mechanical Engineering, National Taiwan University, Taipei, Taiwan 106, R.O.C.

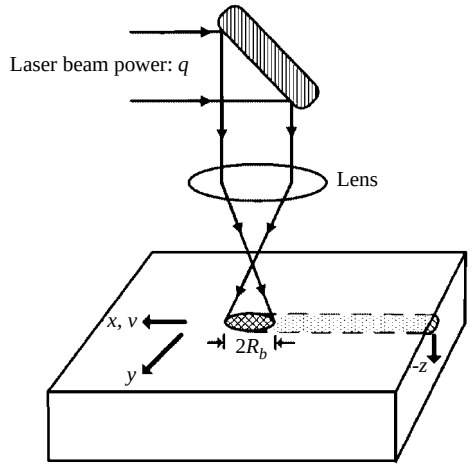

Fig. 1 The geometry and coordinate system of the experiments for the laser beam scanning across a solid surface

thermal properties and easy determination of solutions while it can be used to consider any flux. But still, the results needed complicated calculation. Yet, another approach is that of Bass, who presented temperature field equations for various beam geometries by taking limits to extract analytical results. Ashby and Easterling carried the analytical approach further, developing an approximate solution for the entire temperature field (Ashby and Easterling, 1984). This approach apparently allows easy calculation and is always calibrated by experimental data through comparison with a finite-difference solution and the finite-element method. In this paper, we present a modified Ashby-Easterling heat-transfer model of the laser hardening process in the melt. By inputting the laser processing parameters and the thermo-physical values, this model can be used to predict the surface temperature at which austenization and subsequent martensite transformations occur. In the present study, we have investigated the effect of laser surface hardening on SKD61 steel. We have studied the phase transformations that occurred by using optical and scanning electron microscopic analyses, and have correlated the microstructural behavior with the theoretical temperature profile.

II. MATHEMATICAL MODELING

When a laser beam of power q and radius R_b is tracked in the x direction, with travel speed v, across the surface of a solid (as shown in Fig. 1), the thermal cycle of a point at (y, z) below the surface is T (y, z, t). We assume the solid is large enough that its average temperature T_0 is constant. The energy provided by the laser beam then heats the surface, and the surface is quenched by conduction. In common with other workers in the field, we make the following assumptions

Table. 1 Definitions and units of the symbols used in Eq. 1~4

t	Time(s)
λ	Thermal conductivity (J/m-k)
α	Thermal diffusivity (mm^2/s)
A	Aabsorptivity at the sample surface (0.95, coated with $Mn(H_2PO_4)_2$)
v	Laser travel speed (mm/s)
q	Laser power (W)
R_b	The distance from the Gaussian beam center to the position at which the intensity has fallen to 1/e times the peak value (mm)
T	Temperature (°C)
T_P	Peak temperature (°C)
T_0	Initial temperature defined as room temperature (25°C)
t_m	Melting temperature of SKD61 (°C)
L	Latent heat of melting (J/m^3)
t_0	$R_b^2/4\alpha$, time constant (s)
z_0	Length constant ,given by eq. 1, eq. 2 and eq. 3
z_m	Melted depth by optical microscope measurement
q^*	Power input available to raise the temperature of the remaining solid when melting
A_m	Area of melted zone (mm^2)

(Arata and Inoue, 1986; Ashby, 1985; Ashby and Shercliff, 1991):

1. The surface absorptivity, A, is constant, and the latent heat of transformation is negligible when compared to the other terms in the heat-flow equations.
2. The melting point, latent heat of melting, thermal conductivity, and diffusivity are all constant.
3. The austenized temperature of SKD61 for traditional quenching is 1010°C as given by the TTT diagram (Roberts and Cary, 1980), and the radius R_b of a Gaussian beam is the distance from the beam center to the position at which the intensity has fallen to 1/e times the peak value.

We calculate the temperature changes that occur outside the area of the laser beam impact by using the Ashby-Easterling heat-transfer equation. There we show that the proper solution to the equation of heat flow is well approximated by a simple analytical equation for T (y, z, t) given by

$$T - T_0 = \frac{Aq}{2\pi\lambda v[t(t+t_0)]^{1/2}} \times \exp\{\frac{-1}{4\alpha}[\frac{(z+z_0)^2}{t} + \frac{y^2}{(t+t_0)}]\} . \quad (1)$$

The symbols used in this equation are defined in Table.1. T is the temperature of a point (y, z) at laser treated time t. A is the absorptivity at the sample surface. The symbol q is the laser input power and v is laser travel speed. λ is thermal conductivity and α

is thermal diffusivity. This equation contains two reference parameters. The first, t_0, is a characteristic heat transfer time, defined by $t_0 = R_b^2/4\alpha$. The constant t_0 measures the time for heat to diffuse over a distance equal to the beam radius. The second, z_0, is a characteristic length for correlating the theoretical calculation and experimental findings. The constant z_0 measures the distance over which heat can diffuse during the beam interaction time. It is chosen in a way that gives the correct surface temperature for all q, v and R_b. The function of z_0 is to limit the surface temperature to a finite value. The true surface is taken to be a distance z_0 below the model surface; we evaluated it by matching our solution at $z = z_0$ to known solutions for the surface temperature.

For correlating the theoretical calculation and experimental findings, we have to determine the peak temperature that reaches the maximum temperature during the laser treated time ($t = R_b/v$). The peak temperature field T_P (y, z) is given by

$$T_p - T_0 = \frac{Aq}{2\pi\lambda v[(R_b/v)(R_b/v + R_b^2/4\alpha)]^{1/2}} \times \exp\{\frac{-1}{4\alpha}[\frac{(z+z_0)^2}{R_b/v} + \frac{y^2}{(R_b/v + R_b^2/4\alpha)}]\} . \quad (2)$$

T_P is the peak temperature at a point (y, z) at laser treated time $t = R_b/v$. The laser heating of SKD61 steel, which has poor thermal conductivity and diffusivity, usually causes a melting layer to form. Therefore, we must change some of the reference parameters in the Ashby-Easterling heat-transfer equation to obtain an expression for the temperature field in the case of laser surface hardening in the melt. The peak temperature field T_P (y, z) is given by

$$T_p - T_0 = \frac{Aq^*}{2\pi\lambda v[(R_b/v)(R_b/v + R_b^2/4\alpha)]^{1/2}} \times \exp\{\frac{-1}{4\alpha}[\frac{(z+z_0)^2}{R_b/v} + \frac{y^2}{(R_b/v + R_b^2/4\alpha)}]\} . \quad (3)$$

We obtain the position of the melt boundary and of the contours at which the peak temperature (T_P) reaches the melting point (1483°C) of SKD61 steel by optical microscope measurement. The value z_m is the melted depth by optical microscope measurement and we assume the peak temperature T_P just reaches 1483°C at $z = z_m$ (as shown in Fig. 2). The details, including a small correction for the heat of fusion, are given below.

When the surface is melted, energy is absorbed as the latent heat of the liquid form. Although this

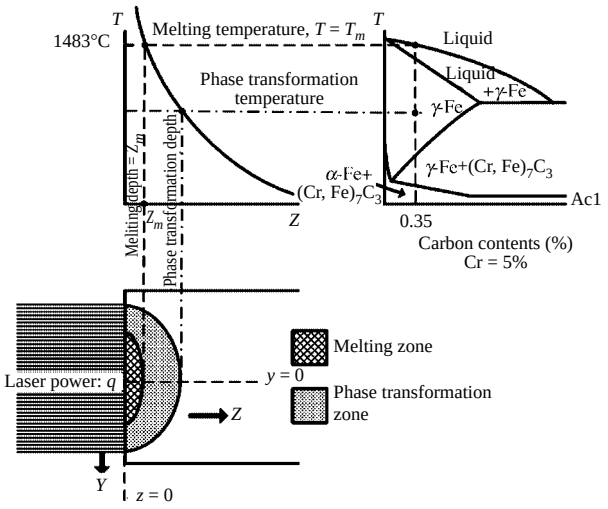

Fig. 2 A physical scheme describing the relation of temperature and phase equilibrium during laser processing of SKD61 steel (C = 0.35%)

energy is released later, it is temporarily removed from the input energy and is not available to melt more material. The energy required for melting per second is $v \times A_m \times L$ and the energy available to raise the temperature of the remaining solid is:

$$q^* = q - v \times A_m \times L. \quad (4)$$

The symbol A_m is the melted area observed by optical microscope measurement. In Eq. (3), z_m, which represents the experimental melting depth, is first approximated as the maximum distance below the center of the laser beam ($y = 0$) that experiences a peak temperature T_P exceeding the melting temperature of 1483°C at $z = z_m$ (as shown in Fig. 2). The melting temperature (1483°C) at depth z_m in the solid is then given by the procedure described earlier, with q replaced by q^*. This substitution gives an equation that can be solved for z_0 and be applied to the calculation in the melt case. After the correction of z_0 for the given q, v and R_b respectively, we can estimate the peak temperature T_P at a point (y, z).

III. EXPERIMENTAL PROCEDURE

The material investigated in this study is SKD61 steel. It is of good resistance to heat softening because of its intermediate chromium content and the presence of carbide-forming elements, such as molybdenum, tungsten, and vanadium. Tables 2 and 3 provide the chemical composition and material properties of SKD61 steel (Whan,1990). The specimen of SKD61 steel was machined into a rectangular block (10 mm × 30 mm × 10 mm) for the laser treatment. As shown in Fig. 3, the laser treatment was performed

Table. 2 Chemical composition of SKD61 steel (wt.%)

Steel	C	Cr	Mn	Si	W	Mo	Ni	V	Fe
SKD61	0.35	5.2	0.3	0.95	1.2	1.35	0.25	0.43	Bal.

Table. 3 Thermo-physical parameters of SKD61 steel (Whan, 1990; Roberts and Cary, 1980)

Properties	Value
Thermal conductivity, λ	28.6 J/m-k
Thermal diffusivity, α	5.35 mm^2/s
Density, ρ	7.76 g/cm^3
Latent heat for melting, L	2.1×10^9 J/m^3
Heat capacity, c	688.4 J/kg-k
Austenized temperature for traditional quenching	1010°C
Melting point, T_m	1483°C

using a 2.0-kW continuous wave CO_2 laser. To focus the beam, we used a Zn-Se lens having a focal length of 190.5 mm. The laser power and travel speed in the experiments were in the ranges of 150-250 W and 10-25 mm/s, respectively, at a beam diameter of 2 mm. To produce oxide-free coatings in all experiments, the laser was shielded using 0.1 MPa N_2 gas. Prior to laser treatment, the surface of the specimen was coated with $Mn(H_2PO_4)_2$ to increase the energy absorption. The hardened specimen was cut perpendicular to the scanning direction, polished, etched in 5% Nital, and then went through microstructure observation. We observed the phase transformations through optical and scanning electron microscopic analyses. The depth of the laser-affected layer was measured using a micro-hardness tester.

IV. RESULTS AND DISCUSSION

Figure 4 indicates that the depth of the melted

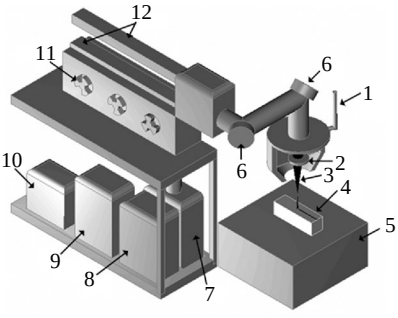

1. N_2 gas inlet
2. Focusing lens
3. Laser beam
4. Specimen
5. CNC worktable
6. Mirror lens
7. Vacuum pump
8. Controller
9. Voltage regulator
10. Converter
11. CO_2 gas circulatory system
12. High-voltage power electrode

Fig. 3 Laser treatment system

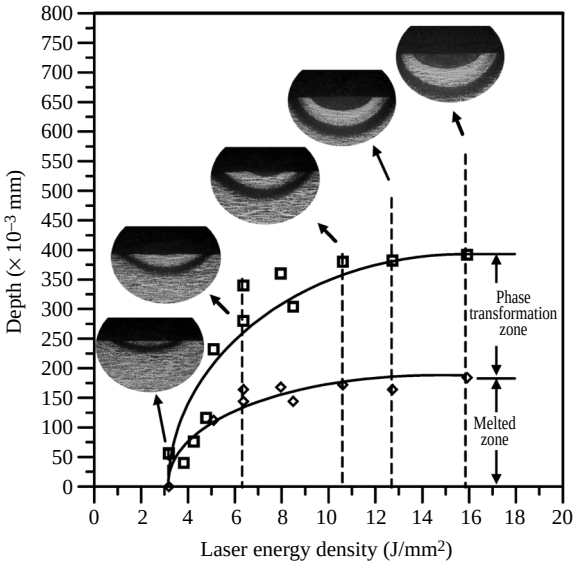

Fig. 4 The depth of the melted zone and phase transformation zone of laser treated quenched SKD61 steel under different laser energy densities

and phase transformation zone of the laser-treated, quenched SKD61 steel increase substantially with increasing laser energy density. The laser energy density is a combination of the laser power, beam diameter, and travel speed, and is defined by Eq. (5).

$$E(Laser\ Energy\ Density) = \frac{4}{\pi} \times \frac{q(Laser\ Power)}{D(Laser\ Beam\ Diameter) \times v(Laser\ Travel\ Speed)} \quad (5)$$

Figure 5 indicates that the depth of the phase transformation zone in the quenched and as received SKD61 steel increase with increasing laser energy density. The depth of the phase transformation zone in the quenched SKD61 steel is substantially higher than that in the base SKD61 steel under the same laser energy density. Compared with the quenched SKD61 steel that presents a structure of martensite, the base steel (SKD61) presents a more heterogeneous structure with metallic carbides dispersed in the matrix. For the laser transformation hardening, the base SKD61 steel needs a higher temperature or longer duration than the quenched SKD61 steel to allow phase transformation to happen.

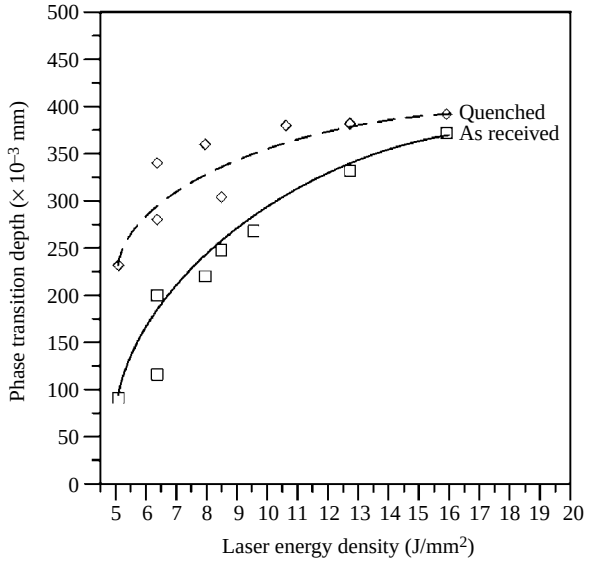

Fig. 5 The depth of the phase transformation zone of laser treated SKD61 steel in the quenched and the as received condition under different laser energy densities

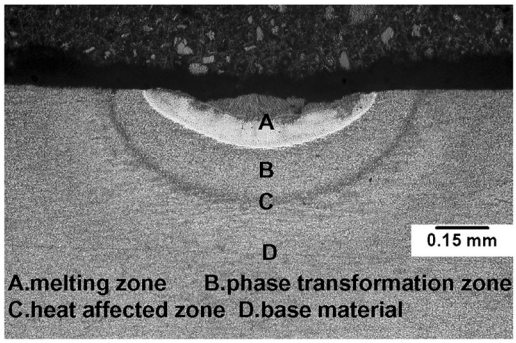

Fig. 6 The cross-section of the laser treated SKD61 base steel with surface melted under the laser energy density of 12.7 J/mm^2

Figure 6 displays the microstructure of laser-treated base SKD61 steel with melted surface. We observe several significantly different characteristics in the evolution of the microstructure in the laser-affected layers by SEM as shown in Fig.7. When the laser is moved away, the melted zone begins to solidify. The self-cooling rate in the liquid state is so high that a dendritic structure is formed as shown in Figs. 7(a) and (b). Figs. 7(b), (c) and (d) are characterized by martensite with metallic carbides precipitated at the grain boundary. In the heat-affected zone as shown in Fig. 7(e), the maximum temperature remains below the austenized temperature and the metallic carbides become larger and more numerous as a result of tempering. The base steel (SKD61) presents a spheroidal structure with metallic carbides dispersed in the matrix, as indicated in Fig. 7(f).

Figure 8 presents the temperature distribution field obtained by using the modified Ashby-Easterling heat-transfer equation (Eq. (3)) and the optical microscopic image. Fig. 8 also presents the comparision of the temperature distribution field by theoretical calculation with the image observed by optical microscope. We note that the contour of 1483°C (melting point) fits better than the contour of 1228°C (phase transformation temperature), when they are compared with the experimental finding (observed by optical microscope). When the laser is moved on, the phase transformation temperature of SKD61 is raised to higher than the austenized temperature of 1010°C for traditional quenching because the heating rate during laser processing is usually greater than 10^4°C/s. This phenomenon is called superheating and it depends on the structure of the steel. The larger the grain size and/or the more heterogeneous the structure, the higher the temperature and/or the longer the duration is required for the phase transformation.

Figure 9 presents the temperature distribution fields obtained by using the modified Ashby-Easterling heat-transfer equation (Eq. (3)) for laser surface hardening of the quenched SKD61 steel under different laser energy densities. Melting occurs below the melted layer within the diagonal crossed line region. The diagram displays temperature contours along which the temperature just reaches the phase transformation temperature of SKD61 steel as shown in the spotted region. Figs. 9(a-d) demonstrate that the critical phase transformation temperature will decrease from 1247 to 1213, 1172, and 1122°C with increasing laser energy density from 5.1 to 8.5, 12.7, and 15.9 J/mm^2, respectively. We observe that the phase transformation temperature in the spotted area of SKD61 steel decreases with increasing laser energy density. This finding implies that when the laser energy density decreases, the temperature will be higher and the duration will be longer for the microstructure of SKD61 steel to transform into austenite. Typically, a minimum interaction time of 10^{-2} s, a power density greater than 10 W/mm^2, and a traverse speed of 5-50 mm/s are required for the transformation hardening of steels, but the temperature should be high enough and the duration long enough for SKD61 steel to transform into uniform austenite. For high-alloy tool steels, the quenching temperature should be higher than the austenized temperature, and the duration should be long enough for carbides to be dissolved into the matrix. Therefore, the temperature of the surface layer during laser hardening of SKD61 steel should be higher than the austenized temperature of 1010°C in traditional quenching. Following this logic, the temperature of the surface layer should be high enough for quenching so that it will enable the complete transformation of austenite into

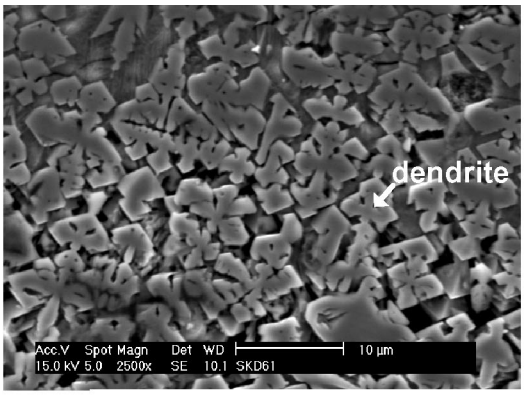

(a) Melted zone

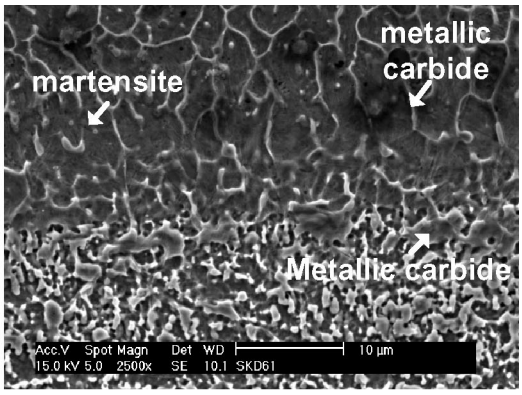

(d) Phase transformation zone+heat affected zone

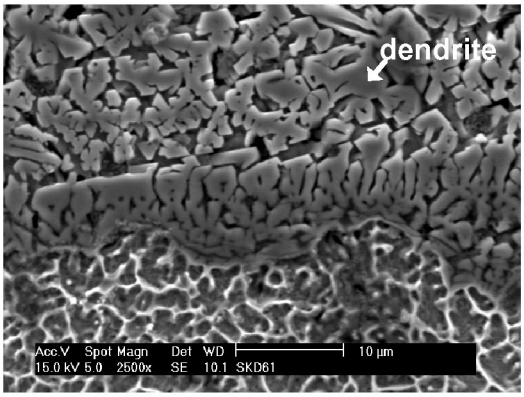

(b) Melted zone+phase transformation zone

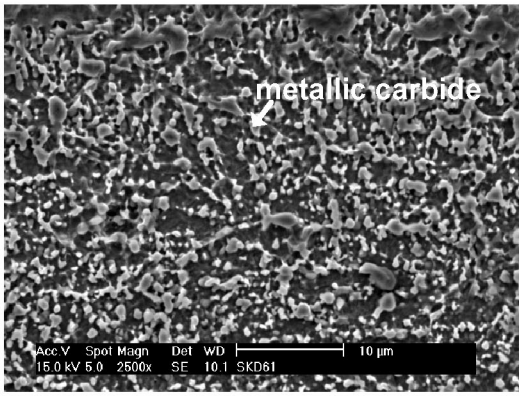

(e) Heat affected zone

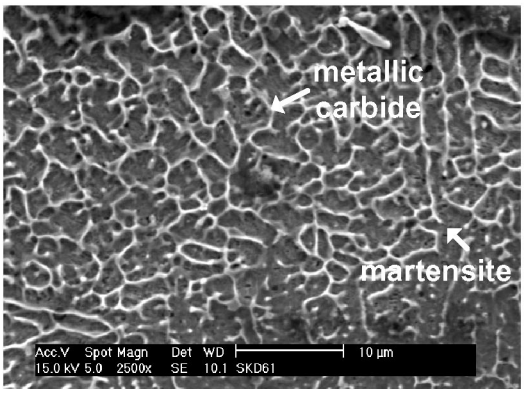

(c) Phase transformation zone

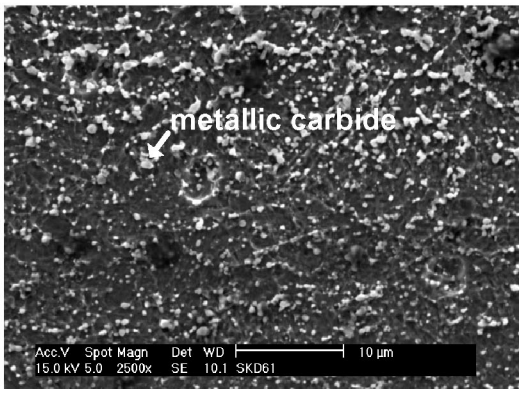

(f) Base material

Fig. 7 SEM analysis of the laser treated base SKD61 steel with surface melting under the laser energy density of 12.7 J/mm^2

martensite (Shiue and Chen, 1992; Bradley and Kim, 1988).

Figure 10 presents the temperature distribution in the surface layer obtained by using the modified Ashby-Easterling heat-transfer equation (Eq. (3)) for the laser surface hardening of SKD61 steel under different laser energy densities. This figure demonstrates that the minimum phase transformation temperature decreases from 1247 to 1228 and to 1122°C for the quenched state and that it also decreases from 1366 to 1324 and to 1155°C for the as-received state when the laser energy density increases from 5.1 to 6.7 and to 15.9 J/mm^2, respectively.

We find that the phase transformation temperature of SKD61 decreases with increasing laser energy density; the phase transformation temperature of SKD61 in the as-received condition is higher than that in the quenched condition under the same energy density. This situation exists because the SKD61 steel in the as-received condition presents a spheroidal

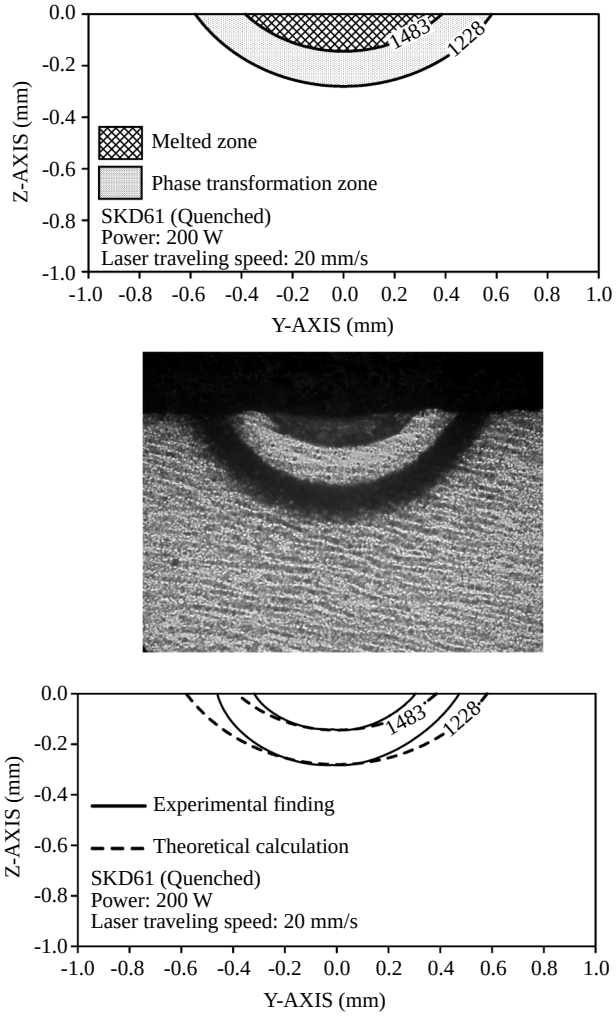

Fig. 8 Comparison of the temperature distribution field simulated by using the modified Ashby and Eastering heat-transfer equation (Eq. 3), and the optical microscopic photo

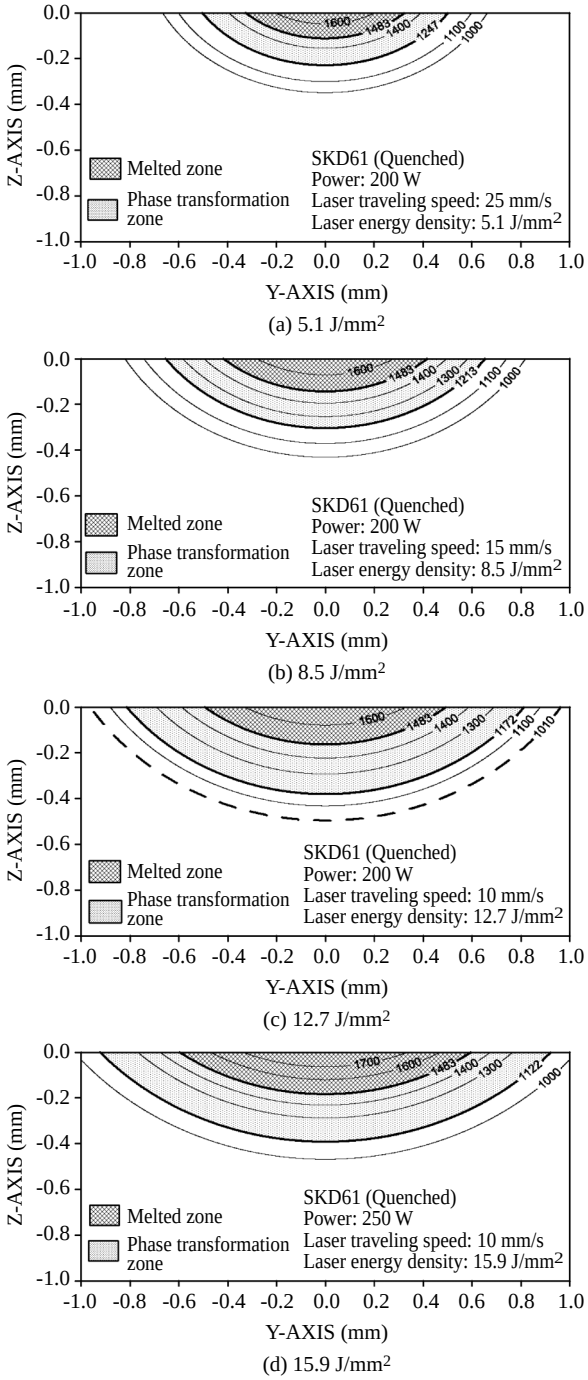

Fig. 9 Temperature distribution field simulated by using the modified Ashby and Eastering heat-transfer equation (Eq. 3) for laser surface hardening of SKD61 steel under different laser energy densities

structure with metallic carbides dispersed in the matrix and, therefore, the temperature should be higher for these carbides to dissolve into austenite and then transform into martensite when transformation hardening occurs.

SKD61 steel contains more than 5 wt% of an additional element, Cr, which attributes to its poor thermal conductivity and diffusivity. Its metallic carbide causes the phase transformation temperature to become higher than the austenized temperature of 1010°C, and it also lengthens the duration time for phase transformation. The Ashby-Easterling heat-transfer equation is not suitable to predict the temperature evolved as it is assumed that the hardening temperature is the austenized temperature of 1010°C during laser heating of the SKD61 steel, even under quenched conditions.

For laser hardening of SKD61 steel, a higher laser energy density brings the phase transformation temperature of SKD61 closer to its austenized temperature of 1010°C in traditional quenching. A comparison of SKD61 steel in its as-received and quenched conditions indicates that the more heterogeneous the structure, the higher the phase transformation temperature is required for SKD61 steel to transform into uniform austenite.

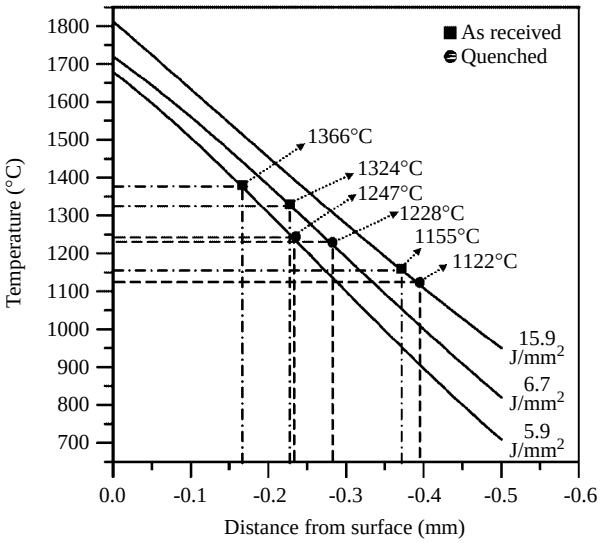

Fig. 10 Temperature distribution from surface and the critical phase transformation temperature calculated by using the modified Ashby and Eastering heat-transfer equation (Eq. 3) for laser surface hardening of SKD61 steel in the quenched and the as received condition under different laser energy densities

V. CONCLUSIONS

There are several significantly different characteristics in the microstructures that evolve in the laser-affected layers of the base SKD61 steel. We note that the basic microstructure in the melted zone is dendrite structure. The phase transformation zone is characterized by martensite with the metallic carbides precipitated at the grain boundary. In the heat-affected layer, the metallic carbides become larger and more numerous as a result of tempering. The base steel (SKD61) presents a spheroidal structure with metallic carbides dispersed in a matrix.

We have applied the modified Ashby-Easterling heat-transfer equation to the laser surface transformation hardening of SKD61 steel. The experimental data indicate that this equation is appropriate to simulate the temperature distribution if we set the temperature of the melt boundary as the melting point of the steel. For laser surface hardening of the SKD61 steel under different laser energy densities, we note that the critical phase transformation temperature of SKD61 steel decreases with increasing laser energy density and that the critical phase transformation temperature of SKD61 in the as-received condition is higher than the corresponding temperature in the quenched condition under the same energy density.

REFERENCES

Arata, Y., and Inoue, K., 1986, *Plasma, Electron and Laser Beam Technology*, ASM, Ohio, USA.

Ashby, M. F., 1985, *Laser Processing of Materials*, AIME, New York, USA.

Ashby, M. F., and Shercliff, H. R., 1991, "The Prediction of Case Depth in Laser Transformation Hardening," *Metallurgical Transactions A*, Vol. 22, No. 10, pp. 438-446.

Ashby, M. F., and Easterling, K. E., 1984, "Transformation Hardening of Steel Surface by Laser beam," *Acta Metallurgica*, Vol. 32, No. 11, pp. 1935-1948.

Bokota, A., and Iskierka, S., 1996, "Numerical Prediction of the Hardened Zone in Laser Treatment of Carbon Steel," *Acta Materialia*, Vol. 44, No. 2, pp. 445-450.

Bradley, J. R., and Kim, S., 1988, "Laser Transformation Hardening of Iron Carbon and Iron Carbon Chromium Steels," *Metallurgical Transactions A*, Vol. 19, No. 8, pp. 2013-2025.

Ganeev, R. A., 2002, "Low-Power Laser Hardening of Steels," *Journal of Material Processing Technology*, Vol. 121, No. 2-3, pp. 414-419.

Goldak, J., Chakravarti, A., and Bibby, M., 1984, "New Finite Element Model for Welding Heat Sources," *Metallurgical Transactions B*, Vol. 15, No. 2, pp. 299-305.

Kou, S., Sun, D. K., and Lee, Y. P., 1983, "Fundamental Study of Laser Transformation Hardening," *Metallurgical Transactions A*, Vol. 14, No. 4, pp. 643-653.

Mazumder, J., Steen, W. M., 1980, "Heat Transfer Model for CW Laser Material Processing," *Journal of Applied Physics*, Vol. 51, No. 2, pp. 941-947.

Olaineck, C., and Luehrs, D., 1996, "Economic and Technical Features of Laser Camshaft Remelting," *Heat Treatment of Metals*, Vol. 23, No. 1, pp. 17-19.

Shiue, R. K., and Chen, C., 1992, "Laser Transformation Hardening of Tempered 4340 Steel," *Metallurgical Transactions A*, Vol. 23, No. 1, pp. 163-170.

Steen, W. M., 2003, "Laser Material Processing - An Overview," *Journal of Optics A: Pure and Applied Optics*, Vol. 5, No. 4, pp. S3-S7.

Whan, R. E., 1990, "Properties and Selection: Irons, Steels, and High-Performance Alloys," *Metals Hand Book*, ASM, OH, USA, Vol. 1, pp. 758-79.

Yang, L. X., Peng, X. F., and Wang, B. X., 2001, "Numerical Modeling and Experimental Investigation on the Characteristics of Molten Pool during Laser Processing," *International Journal of Heat and Mass Transfer*, Vol. 44, No. 23, pp. 4465-4473.

Roberts, G., and Cary, R. A., 1980, *Tool Steels*, ASM, OH, USA.

Manuscript Received: Sep. 21, 2004
Revision Received: Aug. 09, 2005
and Accepted: Sep. 19, 2005